Spatial distribution of reaction products in positive tone chemically amplified resists

Gerard M. Schmid and Michael D. Stewart
Department of Chemical Engineering, The University of Texas at Austin, Austin, Texas 78712

Vivek K. Singh
Intel Corporation, Hillsboro, Oregon 97124

C. Grant Willson[a]
Department of Chemical Engineering, The University of Texas at Austin, Austin, Texas 78712

(Received 14 June 2001; accepted 5 November 2001)

The perpetual advancement of materials and equipment for microlithography has resulted in the ability to print critical dimensions that approach the size of the molecules that make up photoresists. As a result, molecular scale effects such as line edge roughness have become a concern for both resist manufacturers and process engineers. In this work we have investigated the increasing importance of molecular level effects, especially in terms of the contributions of the exposure and postexposure bake (PEB) steps to spatial variations in film composition. A mesoscale simulation of the PEB was used to model the discrete mass transport and reaction events that create the changes in film composition responsible for resist function. Local irregularities in resist composition are generated during the PEB, the magnitude of which can be related to the local concentration of acid. This study is focused on the establishment of an understanding of the effects of process and composition variables on the reaction product distribution. The reaction product distribution was calculated for an APEX®-like resist under a variety of exposure and bake conditions. These process variables have a profound influence on spatial irregularities in the composition gradient. Ultimately, it is the interaction of this reaction product distribution with the development process that will determine line edge roughness. © *2002 American Vacuum Society.* [DOI: 10.1116/1.1431954]

I. INTRODUCTION

The continued reduction in size of resist features has necessitated a concomitant reduction in the error budget for critical features. As lithography enters the 100 nm node, aberrations in feature topography that are on the same length scale as a single polymer can now consume a significant portion of the error budget. The increasing importance of feature roughness at this scale has prompted a significant effort to investigate its origins and ways to reduce it. Many factors have been identified that contribute to feature roughness, including both resist properties and processing conditions. Researchers have investigated the effect on roughness of resist properties including the molecular weight and polydispersity of the resin,[1,2] phase separation or aggregation of resin molecules,[3,4] the presence of base additives,[5,6] and crosslink density in negative tone resists.[7] Processing conditions have also been found to influence feature roughness, including aerial image effects,[2,6,8–10] bake conditions,[8,11] transfer of roughness from the reticle,[12] stochastic effects that occur during dissolution,[13] and ultrasonic development assistance.[14] A variety of computer simulations have also been employed to investigate feature roughness.[15–17] In the work presented here, a mesoscale lithography simulation is used to investigate some of the factors that contribute to feature roughness in positive tone chemically amplified resists.

The validity of treating the resist film as a continuum material during postexposure bake (PEB) and development simulations is arguable. In the early days of lithography simulation, the goal was to predict changes in 3-μm-wide features in 1.5-μm-thick novolak films. For comparison, a novolak monomer is approximately 1 nm in diameter, and the radius of gyration of a typical novolak chain is approximately 3–5 nm. These dimensions effectively define the minimum "pixel size" of the photoresist, so the finest structure in the developed photoresist feature has to be on this length scale. In novolak photoresists, the effect of each individual molecule is generally small because the molecules are several orders of magnitude smaller than the final resist feature dimensions that can be printed with these resists. Molecular level effects can be ignored in this case, and the photoresist topography can be determined appropriately by using a fairly coarse calculation grid ($\sim$50 nm). On the other hand, today's lithographic techniques produce 150-nm-wide features in 300-nm-thick films of resists like poly(p-hydroxy-co-t-butoxycarbonyloxy)styrene. The diameter of a resist monomer is still around 1 nm, and the radius of gyration of a typical chain is approximately 3–5 nm. However, the reduction in feature size leads to a situation in which individual molecules can have a significant effect on the structure of the final photoresist feature. These effects are lost when a continuum approximation is used, on any size calculation grid.

One may readily imagine how the finite size of a polymer molecule can impact the line-edge roughness of the devel-

[a]Author to whom all correspondence should be addressed; electronic mail: willson@che.utexas.edu

oped photoresist feature. The situation is analogous to the case of representing an image with pixels: many small pixels are better at producing a smooth image than fewer large pixels. Developing a photoresist does not produce a gray scale; rather, it is a binary process in which each polymer molecule either remains in the film or dissolves into the developer. Whether or not a given polymer chain will dissolve is dependent upon a number of formulation and processing variables. Prior to the (PEB), the polymer chains that compose a positive-tone chemically amplified resist film are all ostensibly insoluble. This insolubility results from the presence of a number of pendant blocking groups on the polymer chains. In a typical photoresist formulation, blocking 20%–30% of the repeat units on a given chain is sufficient to render that chain insoluble on the time scale of the development process. Illumination of the photoresist through a mask generates acid in exposed regions. At the elevated temperature of the PEB, the acid catalyzes thermolysis of the blocking groups. The end effect is that in regions of high acid concentration, most of the blocking groups are removed and the polymer is very soluble. Similarly, in regions of low acid concentration, most of the blocking groups remain and the polymer is insoluble. In the boundary region between these two extremes lies the variation in polymer solubility that determines the shape of the resist feature after development.

Line edge roughness is the consequence of the complex interaction between the spatial variation in composition that results from exposure and PEB, and the solubility function that describes the action of the developer on that compositional distribution. The first step in understanding line edge roughness is accurate establishment of the spatial variation in the molecular level composition after exposure and baking. In this work a mesoscale model was used to calculate the effect of acid concentration on the compositional distribution produced during the PEB. Lattice models of photoresist films were exposed to produce a variety of acid distributions, and a PEB simulation was used to determine the resulting distribution of blocked polymer sites that is instrumental in determining the topography of the developed resist feature. The final resist image is also strongly dependent on the development process, and the reader is referred to the literature for a detailed discussion of issues affecting photoresist dissolution.[18–22]

II. MESOSCALE LITHOGRAPHY MODELING

Our approach to lithography modeling is based upon the discretization of the photoresist film into cells on a three-dimensional lattice (Fig. 1). Each lattice cell occupies the same volume as a monomer repeat unit of the photoresist polymer. Lattice cells are strung together to form chains, and pendant groups are attached to some sites on the chains to represent the partial blocking of the photoresist resin. Some lattice cells contain photoacid generators (PAGs) and some contain photoproducts (acid plus counterion). Base additives (acid quenchers), residual casting solvent, and other additives can also be included, but in this work they were omitted for simplicity. Vacancies in the lattice represent the free volume of the polymer film. All of the lattice occupants were introduced in amounts that are representative of the concentrations found in the particular photoresist that was being simulated. During the simulation steps, each lattice occupant behaves in a manner consistent with its chemical identity. In this way it is possible to use the simulation to investigate the effects of the various constituents of the resist on the lithographic performance. Among the many formulation variables that may be examined in this manner are polymer molecular weight and polydispersity, PAG loading, and residual casting solvent concentration. The main topic that will be discussed here is the role of acid concentration in the creation of irregularities in the reaction product distribution.

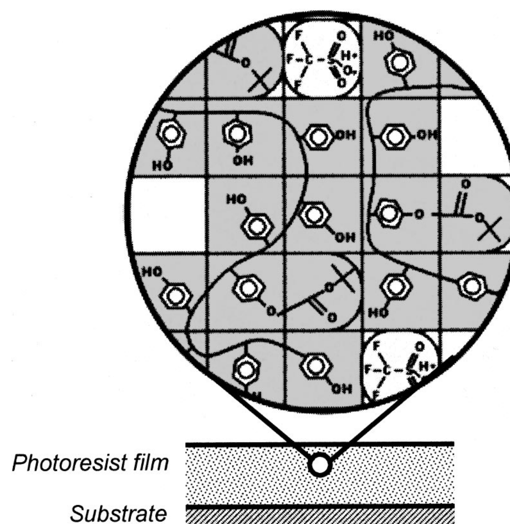

FIG. 1. Lattice representation of a resist film, where every molecule is considered individually. This example is two-dimensional and contains tens of cells. A lattice used in simulation is three dimensional and may contain millions of cells.

A. Generation of a lattice representation of a resist film

The lattice model of the resist film is based upon fundamental and measurable parameters that define the composition of the photoresist. To specify the polymer component, the average degree of polymerization and the standard deviation of the distribution of degree of polymerization must be input. These data can be calculated from the molecular weight distribution of the photoresist resin, which is measurable by techniques such as size exclusion chromatography. It is also necessary to know the average fraction of the polymer repeat units that are blocked, which can be determined by thermogravimetric analysis. These three variables effectively define the photoresist polymer as it is represented on the lattice. The presence of other photoresist components, most notably the PAG loading, must also be quantified. Techniques for measuring such resist properties have been described in the literature.[23–25]

Knowledge of the chemical composition of the photoresist allows one to calculate the appropriate population of each component in the lattice. Each component can then be added sequentially until the desired concentration is present

in the lattice. In the first step of lattice creation, straight chains are added to the lattice by stringing cells together to the desired chain length and chain length distribution. These chains are then equilibrated via many simulated reptations that have the effect of introducing bends into the chains and eventually randomizing their conformation.[26] In the next step, pendant groups are added to random positions on the chains to represent blocked sites on the polymer chains. Finally, PAG molecules are added by randomly converting lattice vacancies into PAG units until the required concentration of PAG has been created.

B. Mesoscale exposure simulation

Once the lattice is configured, it is exposed by selectively converting the PAGs into acids on the basis of their location within the photoresist film. To this end the commercial lithography simulation package PROLITH 7® was used. This software is capable of calculating the energy deposited into any volume element of the resist while varying the exposure wavelength and partial coherence, the numerical aperture of the imaging system, conventional, annular, and quadrupolar illumination schemes, and arbitrary mask structures (including phase shifts), among many other processing variables. The result of the exposure calculation was a deposited energy distribution throughout the resist film, which was then converted into the fractional conversion of PAG as a function of location within the film based upon knowledge of the local energy and the measured quantum efficiency of the PAG. In this way, a continuous distribution of energy is converted into a discrete distribution of acid in the mesoscale simulation.

C. Mesoscale PEB simulation

During the PEB simulation, all single-cell lattice occupants (e.g., PAGs and acids) are allowed to move via a random walk through the vacant cells of the lattice. During this process, some acid molecules come into contact with blocking groups with which they may chemically react. When an acid unit comes into contact with a blocking group it catalyzes the removal of the pendant group. In the actual resist, the volatile cleavage products generally leave the resist film as gases. This process was modeled in the lattice simulation by removing the blocking group from the polymer chain, to produce a temporary void in the lattice.

III. SIMULATION RESULTS AND DISCUSSION

A. Generation of a lattice representation of a resist film

The results presented in this work were generated from a lattice that is 144 cells in each of the three dimensions, corresponding to a volume of approximately $(100\ \text{nm})^3$. This lattice was filled with monodisperse chains 35 repeat units long and equilibrated by a simulated reptation process.[26] In the reptation process, an entire chain may undergo snakelike motions if a void is present near one end of the chain. This process is repeated many times and has the ultimate effect of randomizing the conformations of the chains. The mean squared radius of gyration and mean squared end-to-end distance were monitored during the equilibration process. The lattice was considered to be at equilibrium when lattice properties no longer changed with further equilibration steps (Fig. 2). For long chains, the ratio of the mean squared end-to-end distance to the mean squared radius of gyration has been calculated to have a value of 6.[27] As can be seen in Fig. 2, simulation results agree well with this predicted value. After equilibration, pendant groups were added to random locations on the polymer chains to represent the blocked fraction of polymer sites. The distribution of blocking fractions was Gaussian, with a mean of 0.30 and a standard deviation of approximately 0.10 (Fig. 3). Photoresists typically consist of random copolymers, so this distribution of blocking fractions is an accurate representation of what would be found in an actual resist. The last step in creating the film was to add PAG molecules to the lattice by randomly converting a fraction of the voids into PAGs. This was done

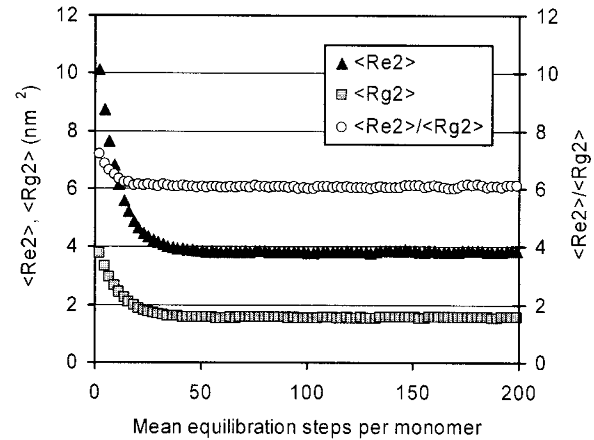

FIG. 2. Equilibration of the polymer chains. The mean-squared end- to-end distance ($\langle R_e^2 \rangle$) and the mean-squared radius of gyration ($\langle R_g^2 \rangle$) are periodically calculated.

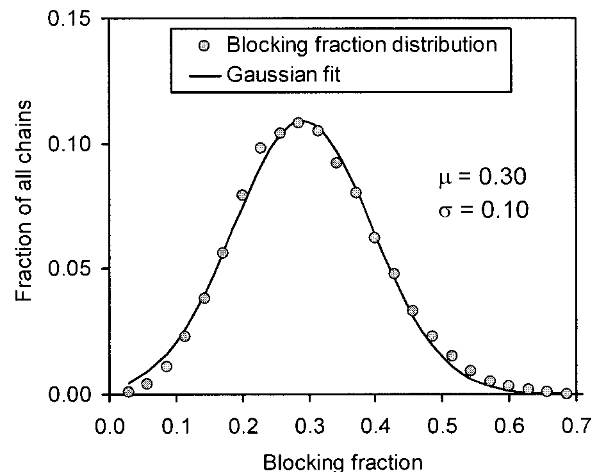

FIG. 3. Blocking fraction distribution of the simulated photoresist polymer.

such that the number ratio of polymer sites to PAG sites was 20:1, leaving 10% of the lattice vacant to represent the available free volume in the polymer film. At this stage the lattice model represents a $(100\ \mathrm{nm}\times 100\ \mathrm{nm}\times 100\ \mathrm{nm})$ volume of an APEX®-type photoresist film.

B. Evaluation of catalytic effect per acid

The high sensitivity provided by chemically amplified resists is a result of the catalytic action of the photoproducts. A single acid molecule produced during exposure can cause many reactions that alter the solubility of the resist film. However, an acid molecule can only cause reactions if reactive material is present nearby. Each acid must therefore undergo a certain degree of translational motion in order to continue to react. In this respect, acid transport is desirable in that it allows a single photogenerated acid to alter the solubility of a larger portion of the resist film. On the other hand, transport of acid into unexposed regions of the resist film complicates control over feature dimensions.[28,29] To more fully understand how acid molecules near the nominal feature edge affect the final topography, we performed several simulations of feature edges. These simulations all focus on a $(100\ \mathrm{nm}\times 100\ \mathrm{nm}\times 100\ \mathrm{nm})$ resist volume that is centered around the nominal feature edge of an individual line in an array of 100 nm equal lines and spaces.

The influence of an individual acid molecule in determining the shape of the resist feature is related to the number of reactions that it catalyzes during the PEB and to the location of those reactions. The number of reactions that are catalyzed during the PEB has been taken as a single fixed quantity or constant in several analyses, but this is an oversimplification of a complex mechanism. As it happens, the location of an acid molecule strongly determines the number of reactions that it can catalyze. Consider an acid molecule that is generated in the center of the exposed region of the resist film. Due to the high exposure in this region, a large number of PAG molecules will be converted into acids, and the deprotection reaction will therefore proceed very quickly in this volume. All of the reactive material (blocked sites) in this volume will be rapidly depleted, whereupon the reactions will cease. Now consider an acid molecule that is generated in the tail of the aerial image. Very few acid molecules are present in regions of such low exposure, and so the reaction proceeds more slowly. It is therefore possible for an individual acid in a region of low acid concentration to continue to cause deblocking reactions long after all blocked sites are gone in the regions of high acid concentration.

If the volume of resist that each acid molecule contacts is assumed to grow spherically, then it is easy to conceptualize that these volumes of influence will overlap quickly in regions of high acid concentration, as shown in Fig. 4. In regions where acid molecules are sparsely distributed, the volume of influence must be considerably larger before another reacted region is encountered. There is less volume of resist available *per acid* in regions of high acid concentration. (It should be noted that the volume of acid influence does not actually grow spherically during the PEB, but rather takes a more tortuous path as the acid moves through the film. The volumes have been depicted as spheres only for clarity of illustration.)

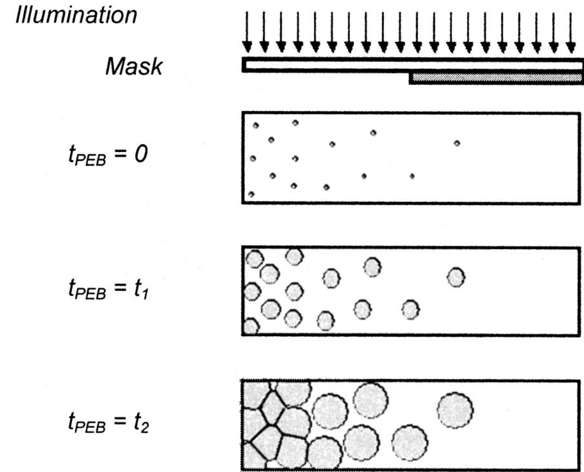

FIG. 4. During the PEB, volumes of acid influence quickly overlap where there are high concentrations of acid. In this two-dimensional cartoon, the volume of influence has been depicted as a circle. In actuality, the acid follows a more tortuous path as it moves through the resist film.

To quantify this effect, simulations of line edges were performed for the exposure conditions shown in Fig. 5. Three sinusoids were used to simulate exposure conditions with varying image slopes. PAG in the lattice was converted to acid in accordance with each particular exposure condition. A PEB simulation was then performed on each lattice for a total of 5×10^3 simulation steps, during which time the number of reactions catalyzed per acid molecule was tracked. These data have been plotted as a function of the final acid location in Fig. 6. It is clear that the number of reactions that each acid catalyzes is a strong function of location for the different exposure conditions. In locations where there is a high concentration of acid, blocking groups are the limiting reagent. These reactive sites are quickly depleted, and the resulting number of reactions per acid is low

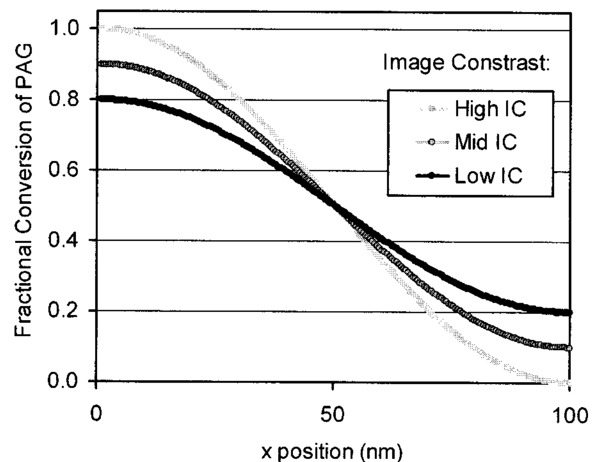

FIG. 5. Exposure conditions used for several line edge simulations. The three cases shown represent a range of different image contrasts (IC).

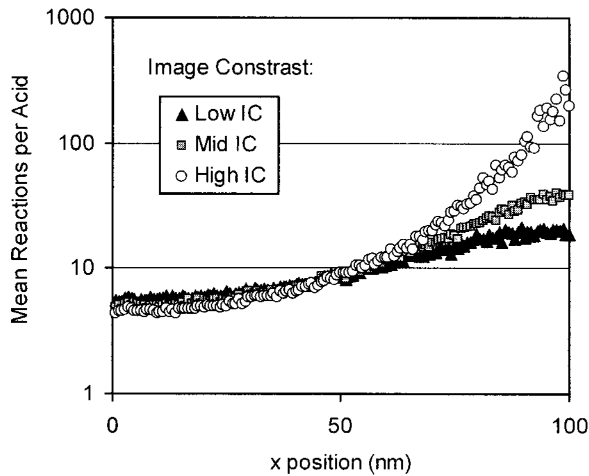

FIG. 6. Mean number of reactions per acid as a function of location for the exposure conditions. Acids that are present in regions of low acid concentration may catalyze many more reactions than acids in regions of high acid concentration.

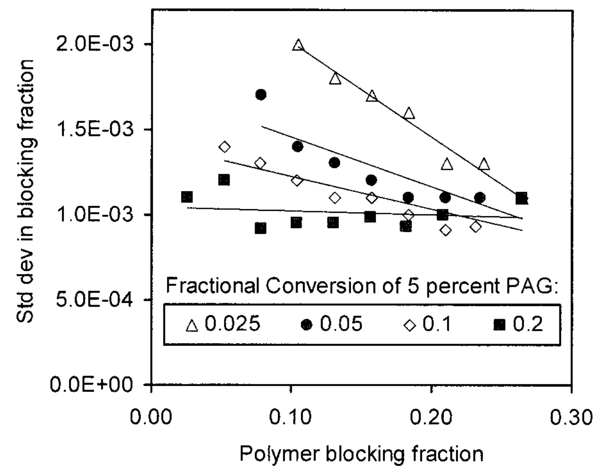

FIG. 7. Spatial irregularity in reaction product distribution: standard deviation of blocking fraction. For equal degrees of deprotection, higher acid concentrations produce smoother distributions (smaller standard deviation).

(<10). In regions where there is a very low concentration of acid, the acids are the limiting reagent. As a result, the number of reactions per acid is much higher in these regions, as shown in Fig. 6. It is therefore misleading to assign a single, average value to the "catalytic chain length" in this sort of reaction analysis.

It should be noted that the location of the feature edge cannot be inferred from the information given in Fig. 4. The location of the feature edge depends on a convolution of the distribution of blocked with a solubility function, not on the number of reactions per acid. This discussion is focused only on quantification of the irregularity in the reaction product distribution. The interaction of this distribution with the development process is the subject of ongoing research studies.

C. Calculation of spatial distribution of reaction products

Complete overlap of the individual regions of acid influence during the PEB produces a volume of the resist that is fully deprotected. It is the regions where the overlap is not complete that determines the final resist topography. The feature edge is defined at the interface between soluble and insoluble regions where the resin protection level has been decreased to the degree that enables dissolution. (This value is dependent upon both the chemical composition of the resist and the development conditions, and is beyond the scope of this work.) However, due to the nature of the deprotection reaction, there are several ways to achieve the same level of deprotection. The same average level of deprotection can be produced by a high concentration of acid and a short PEB or with fewer acid molecules and a long PEB. The mesoscale structure of the reaction product distribution is very different for the two cases.

In a series of simulations, the PAG in the lattice was uniformly converted to several different levels of bulk acid concentration that correspond to the regions of low acid concentration depicted in Fig. 5. A PEB simulation was performed on each lattice, and the three-dimensional reaction product distribution was periodically recorded. To quantify the spatial irregularity in each reaction product distribution, the blocking fraction of the polymer chain that occupies each lattice location was calculated. The mean and standard deviation of the blocking fraction in each lattice have been plotted in Fig. 7 for several different acid concentrations. The blocking fraction of each lattice was identical prior to the PEB. During the PEB, each lattice progressed from higher blocking to lower blocking (right to left in Fig. 7). For equal degrees of deprotection, higher acid concentrations produced smoother distributions of blocking fraction. These smooth distributions can be expected to produce smoother features upon development if the development process is halted at the region of higher acid concentration. The effect can be visualized by simply plotting a two-dimensional slice of the three-dimensional reaction products distribution. This has been done for two blocking fraction distributions in Fig. 8, where dark regions have a lower blocking fraction than light regions. Both of these distributions have an average blocking fraction of 0.156, but the standard deviations vary by almost a factor of 2.

IV. CONCLUSIONS

Simulations have shown that there is significant variation in the number of reactions that each acid molecule catalyzes during the postexposure bake. Acids that are in regions of high acid concentration generally participate in far fewer reactions than acids that are in regions of low acid concentration. It is therefore misleading to refer to a single "catalytic chain length" for a particular photoresist. The feature edge occurs in some region of intermediate acid concentration, but the exact location of the feature edge is ultimately determined by both material properties and development conditions. It is desirable to have the feature edge occur at a relatively high acid concentration, because the simulations suggest that this leads to a smoother composition gradient.

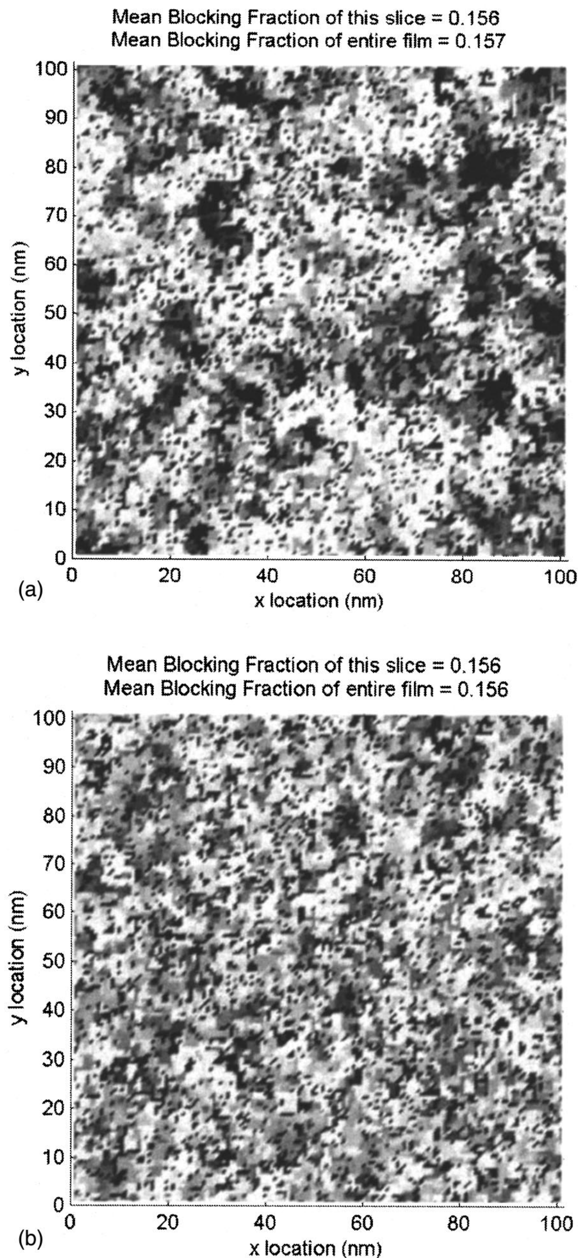

FIG. 8. Slices in the blocking fraction distribution of two lattices. Both lattices have the same average degree of deprotection, but (a) was produced with a longer PEB and fewer acid molecules than (b). For equal degrees of deprotection, higher acid concentrations produce smoother blocking fraction distributions. The fractional conversion of PAG used to produce these blocking fraction distributions was 0.025 for (a) and 0.20 for (b), resulting in standard deviations of 1.7×10^{-3} and 9.8×10^{-4}, respectively.

ACKNOWLEDGMENTS

The authors would like to thank Matthew Stone and Dr. Isaac Sanchez at the University of Texas at Austin for their helpful assistance and advice. This work has been supported by the SRC and DARPA. G.M.S. gratefully acknowledges the Eastman Kodak Corporation for support in the form of a graduate research fellowship.

Presented at the 45th International Conference on Electron, Ion, and Photon Beam Technology and nanofabrication, Washington, DC, 29 May–1 June 2001.

[1]T. Yoshimura, H. Shiraishi, J. Yamamoto, and S. Okazaki, Jpn. J. Appl. Phys., Part 1 **32**, 6065 (1993).
[2]M. I. Sanchez, W. D. Hinsberg, F. A. Houle, J. A. Hoffnagle, H. Ito, and C. Nguyen, Proc. SPIE **3678**, 160 (1999).
[3]Q. Lin, R. Sooriyakumaran, and W. Huang, Proc. SPIE **3999**, 230 (2000).
[4]T. Yamaguchi, H. Namatsu, M. Nagase, K. Kurihara, and Y. Kawai, Proc. SPIE **3678**, 617 (1999).
[5]T. Ushirogouchi, K. Asakawa, M. Nakase, and A. Hongu, Proc. SPIE **2438**, 609 (1995).
[6]E. Shiobara, D. Kawamura, K. Matsunaga, T. Koike, S. Mimotogi, T. Azuma, and Y. Onishi, Proc. SPIE **3333**, 313 (1998).
[7]J. Nakamura, K. Deguchi, and H. Ban, J. Photopolym. Sci. Technol. **11**, 571 (1998).
[8]S. Masuda, X. Ma, G. Noya, and G. Pawlowski, Proc. SPIE **3999**, 252 (2000).
[9]T. Azuma, K. Chiba, M. Imabeppu, D. Kawamura, and Y. Onishi, Proc. SPIE **3999**, 264 (2000).
[10]D. He, H. Solak, W. Li, and F. Cerrina, J. Vac. Sci. Technol. B **17**, 3379 (1999).
[11]D. He, J. Vac. Sci. Technol. B **16**, 3748 (1998).
[12]S. C. Palmateer, S. G. Cann, J. E. Curtin, S. P. Doran, L. M. Eriksen, A. R. Forte, R. R. Kunz, T. M. Lyszczarz, M. B. Stern, and C. Nelson, Proc. SPIE **3333**, 634 (1998).
[13]L. W. Flanagin, V. K. Singh, and C. G. Willson, J. Vac. Sci. Technol. B **17**, 1371 (1999).
[14]S. Yasin, A. Mumtaz, D. G. Hasko, F. Carecenac, and H. Ahmed, Microelectron. Eng. **53**, 471 (2000).
[15]G. Patsis, N. Glezos, and I. Raptis, J. Vac. Sci. Technol. B **17**, 3367 (1999).
[16]G. Patsis, A. Tserepi, I. Raptis, N. Glezos, E. Gogolides, and E. S. Valamontes, J. Vac. Sci. Technol. B **18**, 3292 (2000).
[17]L. Ocola, P. A. Orphanos, W. Y. Li, W. Waskiewicz, A. E. Novembre, and M. Sato, J. Vac. Sci. Technol. B **18**, 3435 (2000).
[18]P. C. Tsiartas, L. W. Flanagin, C. L. Henderson, W. D. Hinsberg, I. C. Sanchez, R. T. Bonnecaze, and C. G. Willson, Macromolecules **30**, 4656 (1997).
[19]L. W. Flanagin, C. L. McAdams, P. C. Tsiartas, C. L. Henderson, W. D. Hinsberg, and C. G. Willson, Proc. SPIE **3333**, 268 (1998).
[20]L. W. Flanagin, V. K. Singh, and C. G. Willson, J. Polym. Sci., Part B: Polym. Phys. **37**, 2103 (1999).
[21]L. W. Flanagin, C. L. McAdams, W. D. Hinsberg, I. C. Sanchez, and C. G. Willson, Macromolecules **32**, 5337 (1999).
[22]A. Reiser, Z. Yan, Y. K. Han, and M. S. Kim, J. Vac. Sci. Technol. B **17**, 1288 (2000).
[23]C. R. Szmanda, R. Kavanagh, J. Bohland, J. Cameron, P. Trefonas, and R. Blacksmith, Proc. SPIE **3678**, 857 (1999).
[24]A. B. Gardiner, A. Qin, C. L. Henderson, S. Pancholi, W. J. Koros, C. G. Willson, R. R. Dammel, C. A. Mack, and W. D. Hinsberg, Proc. SPIE **3049**, 850 (1997).
[25]J. F. Cameron, J. Mori, T. M. Zydowsky, D. Kang, R. Sinta, M. King, J. Scaiano, G. Pohlers, S. Virdee, and T. Connolly, Proc. SPIE **3333**, 680 (1998).
[26]G. M. Schmid, V. K. Singh, L. W. Flanagin, M. D. Stewart, S. D. Burns, and C. G. Willson, Proc. SPIE **3999**, 675 (2000).
[27]K. Kremer and G. S. Crest, in *Monte Carlo and Molecular Dynamic Simulations in Polymer Science*, edited by K. Binder (Oxford University Press, New York, 1995), Vol. 1, p.199.
[28]S. V. Postnikov, M. D. Stewart, H. V. Tran, M. A. Nierode, D. R. Medeiros, T. Cao, J. Byers, S. E. Webber, and C. G. Willson, J. Vac. Sci. Technol. B **17**, 3335 (1999).
[29]J. Sturtevant, S. Holmes, and P. Rabidoux, Proc. SPIE **1672**, 114 (1992).